

Numerical Model of CAI Test for Fibre-Reinforced Polymer Plate

Piotr BASZCZYŃSKI
Sebastian DZIOMDZIORA
Rafał NAZE

*Lodz University of Technology
Stefanowskiego 1/15, Łódź, Poland*

Tomasz KUBIAK
*Department of Strength of Materials
Lodz University of Technology
Stefanowskiego 1/15, Łódź, Poland
tomasz.kubiak@p.lodz.pl*

Received (15 August 2016)

Revised (16 August 2016)

Accepted (17 September 2016)

This article presents numerical simulations of laminates subjected to Compression After Impact (CAI) testing including delamination modelling. Different model of impact damages of laminate were considered. Progressive damage analysis have been employed and different failure criteria have been applied. For each simulation failure load has been estimated as same as the position of damages at destroyed layer. Finally, obtained numerical results were compared with experimental data from referential paper.

Keywords: CAI, numerical simulations, FEM, FRP laminates.

1. Introduction

Together with the development of composite industry, the issue of laminates examination was raised by many researches around the world. The biggest increase in knowledge concerning composites took place in 1960s and 1970s, when the carbon fibre technology was introduced [1].

Numerous analysis concerning composite strength were performed. One of them, was expressed by the idea of examining effects of partial damage of laminate plate. Such a situation may be represented in real situation by a low-velocity impact case (dropping a tool on a composite aircraft wing). At the beginning, carbon fibre reinforced composites were used for modern lightweight structures in aircraft engineering, whereas nowadays it is also convenient material in automotive and civil engineering [1, 2]. At the other hand its brittleness may cause problems as it can

cause significant drop of strength in case of material spot damage.

Normalized test stands were firstly designed in early 1980s by NASA-Langley Research Centre and by The Boeing Co. (Seattle, Wash.). Compression after impact (CAI) testing comprises of two parts: pre-damaging of a specimen with the aid of an instrumented drop weight tester and static compression test for measuring the residual strength. Exemplary experimental stands produced by Zwick/Roell Company may be seen in 2.

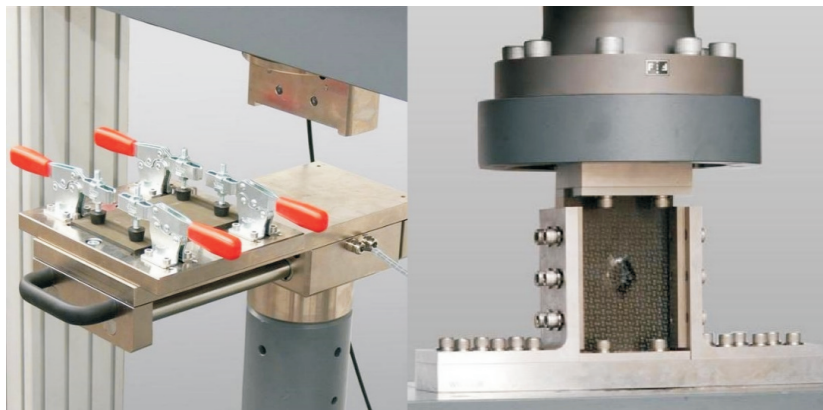


Figure 1 CAI experimental stand produced by Zwick/Roell: a) impacting stand, b) compression fixture [3]

Main idea of the authors of current paper was to create benchmark for the laminates in order to assess how much strength they lose while subjected to impact damage. To do this, Finite Element Method model was created in Ansys Mechanical APDL software basing on experimental data from the article by Sztetek and Olsson [4].

In the available literature it is possible to find many examples of works concerning the analysis of damage after impacting laminate surface and analysis of CAI tests results [4-7]. Those works are mainly focused on the results of physical experiment. Moreover, there are many papers presenting numerical models analysing the damage propagation as the result of impact [8, 9]. Unfortunately, there is a low number of articles concerning numerical models of CAI tests for laminates previously damaged by impact. Taking that into consideration, the authors decided to introduce a simple numerical models of damaged regions formed as a result of impacting with low velocity. Such a model could serve as the basis for CAI simulations by estimating decrease of mechanical properties of the material in the damaged region, as well as analysing stress-strain state. Furthermore, damage propagation paths from damaged region can be also investigated.

2. Numerical model

Numerical model of the investigated problem was built in Ansys environment, based on reference data taken from scientific papers. In the literature there are a lot of

papers dealing with low velocity impact test and CAI test for different type of laminates [4–7]. The authors have decided to take into consideration the paper written by Sztefek and Olsson [4] which provides relevant information about specimen’s shape, material properties, impact energy and approximation of the observed delamination area. The examined sample is a 148x100 mm plate consisting of 16 layers of Hexcel AS4/8552 carbon/epoxy prepreg. Each ply is 0.133 mm thick resulting in 2.14 mm of total laminate thickness. The layup of the plates was [(0/+45/-45/90)_s(90/-45/+45/0)_s] (see Fig. 2). This arrangement is not symmetric, but it was specifically selected in order to obtain a quasi-isotropic behaviour. Nominal ply properties, presented in Table 1 were taken from [4]. More details on the specimen can be found in [4].

Table 1 Material properties of the Hexcel AS4/8552 carbon/epoxy [4]

E_X	E_Y	E_Z	G_{XY}	G_{YZ}	G_{XZ}	ν
123 GPa	10.3 GPa	10.3 GPa	4.73 GPa	4.73 GPa	4.73 GPa	0.3

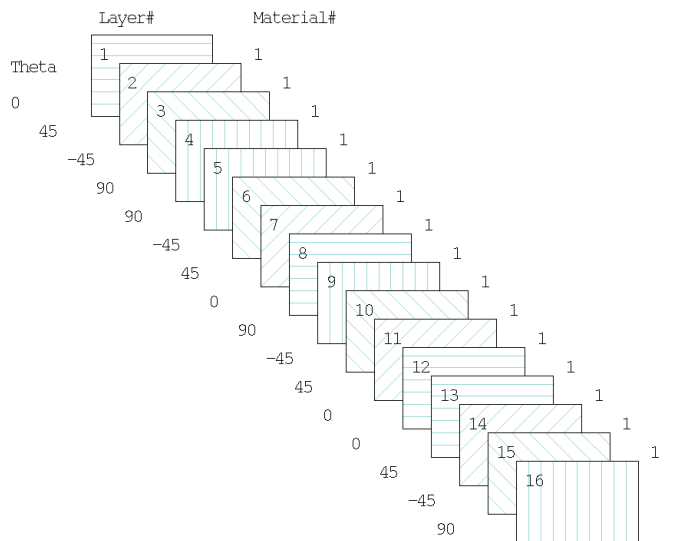


Figure 2 Section lay-up of the investigated plate

The paper [4] covers a number of laminate impacting procedures with different impact energies for two configurations of the plates (16 ply and 32 ply). The study described in this paper is focused on the 16 ply plate impacted with 5J energy. The impacted side (marked as L1 and L16; that abbreviation corresponds to the layer with orientation of fibre direction 0 and 90 degree respectively) was not clearly

stated. It was deduced, based on the orientation of Zg axis in the Fig. 5 of [4], that the laminate is being damaged from side L1. It should be taken into account while evaluating the results because the plate is not symmetric and the impact side might have an influence on its behaviour during compression after impact test. After impacting, plates were examined with use of ultrasonic scanning for detection of a delamination. Results of this procedure for the case examined in this work are presented in [4]. It can be noted that for 5J impact energy, the delaminated area may be approximated by a circle of 14mm diameter (Fig. 3).

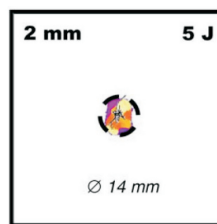


Figure 3 Size of damaged region for 16ply plate impacted with 5J energy [4]

Mechanical properties concerning ultimate strength of the material were not included in the source article paper [4]. Values gathered in Table 2 were taken from [10] and refer to the same material.

Table 2 Ultimate strength of the investigated material for both fiber and matrix [10]

Fibre ultimate tensile strength	1867	MPa
Matrix ultimate tensile strength	26	MPa
Fibre ultimate compression strength	-1531	MPa
Matrix ultimate compression strength	-214	MPa
Ultimate shearing strength	100	MPa

Having defined the size of the interlaminar delamination in the impacted region, the separation between two material layers had to be modelled. There are different modelling techniques available in the ANSYS 15.0 environment, such as Cohesive Zone modelling [11] in order to investigate the growth of the delamination on fracture strength of a composite sample. In the present study, delaminated zone has a predefined size and does not change as a function of the applied compressive force. Consequently, a numerical model was developed with an assumption that delamination occur only between two laminas. Cases having more than one interlaminar delamination cannot be checked using the proposed model.

Such an approach have been assumed in order to prepare simple numerical model which can be applied not only for specimens or small structures but also for big real structures.

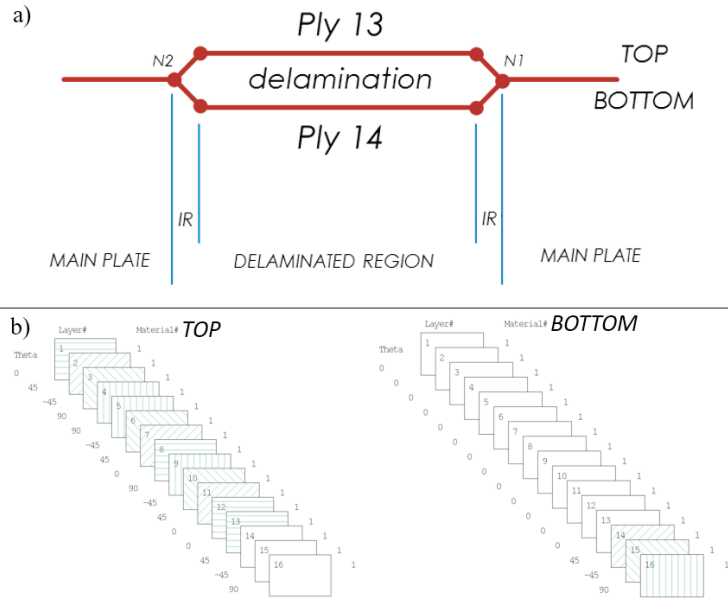


Figure 4 Exemplary case of delamination in the examined plate: a) sectional view of delamination, b) corresponding lay-ups for TOP and BOTTOM sections

For explanation purposes, it is assumed that delamination is present between the 13th and 14th ply of the investigated sample as visualized in Fig. 4a and located in the centre of the sample. Further in this paper, the vertical position of the delamination (referred to as Delamination Position) is counted from the bottom side of the specimen (ply 16, orientation 90). In this region, the split between the laminas is modelled as two separate sections of material (named TOP and BOTTOM) stacked one on top of the other. Their main objective is to reconnect these separated sections to the main plate using common nodes (N1 and N2) located at the circumference of the delaminated zone. It should be noted, that in the numerical model the distance between considered laminas is zero. The exaggeration, as depicted in Fig. 4a, was made to facilitate understanding of the concept of assumed model. The lay-up of the TOP and BOTTOM sections are presented in Fig. 4b. For the former, 13 plies are active (plies from 14 to 16 have zero thickness assigned) while for the later, only 3 have non-zero thickness. Depending on the location of the delamination, the number of plies changes adequately. Adding zero-thickness is not necessary from the point of view of numerical calculations but it facilitates presentation of the results.

The numerical model was built using four-noded shell elements with six degrees of freedom at each node. The boundary conditions were applied at the nodes corresponding to the external circumference of the plate (as shown in Fig. 5). The laminated plate was clamped and boundary conditions imposed the following constraints:

- Edge 1 – $UZ = 0$, $ROTY = 0$, coupling $UX = \text{constant}$;
- Edge 2 – $UZ = 0$, $ROTX = 0$, coupling $UY = \text{constant}$;
- Edge 3 – $UZ = 0$, $UX = 0$, $ROTY = 0$;
- Edge 4 – $UZ = 0$, $UY = 0$, $ROTX = 0$;

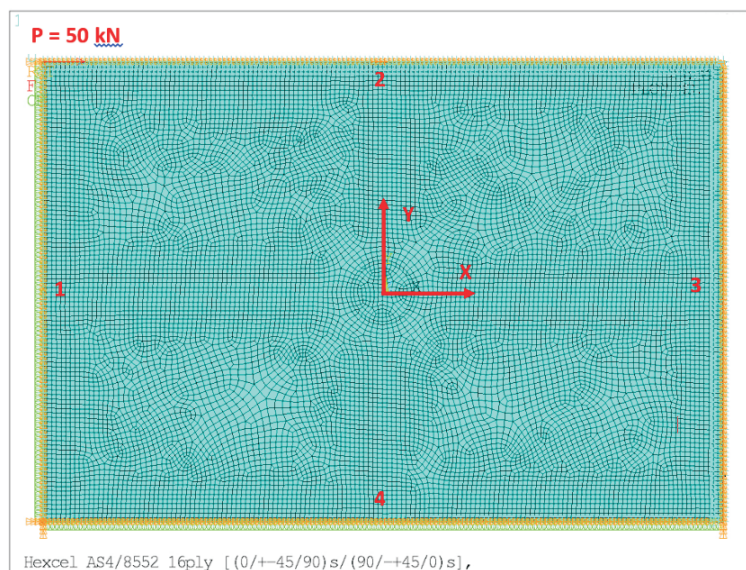


Figure 5 Applied mesh and boundary conditions for the investigated plate with numbers assigned to each edge

Compressive load – force P was applied to the corner node, however due to the coupling UX boundary condition the displacement of edge 1 (see Fig. 5) along X axis is the same for all nodes located on that line. The geometry was meshed with element size equal to 1, what gives c.a. 100 elements in width and 150 elements in length direction.

Once the geometry was defined and all relevant boundary conditions applied, settings for the simulations model were specified. In this investigation, an approach known as Progressive Damage Analysis (PDA) was applied to certain number of tested configurations. It allows to estimate ultimate composite strength under complex loading conditions. The algorithm uses Damage Initiation Criteria (Maximum Stress / Strain, Puck, Hashin, etc.) for determination of damage onset in a given element and reduces stiffness of the element according to data specified by the user (Damage Evolution Law, where 0 = no damage and 1 = complete damage). Consequently, the approach helps to answer the question how many elements have failed under considered loading, but more importantly shows what happens when these

Table 3 Selected parameters for the Progressive Damage Analysis [14]

	<i>Fibre tension</i>	<i>Fibre compression</i>	<i>Matrix tension</i>	<i>Matrix compression</i>
<i>Damage Initiation Criterion</i>	Hashin	Max Stress	Puck	Puck
<i>Damage Evolution Law</i>	0.9	0.9	0.8	0.7

elements are failing. Parameters and criteria selected for this study are presented in Tab. 3.

The Newton–Raphson method was implemented to solve the investigated non-linear problem. Number of sub-steps was set to 100 and data was recorded every two substeps (i. e. 1kN). Due to stabilization the numerical problems in the final steps of the solution, damping factor DF of 0.01 was included in the analysis. The numerical damping factor is the value that software uses to calculate stabilization forces for all subsequent steps and is connected with the concept of energy dissipation [12].

As the main objective of this study was to create simple numerical model in order to investigate laminate behaviour during CAI testing. During preparation and validation of the numerical model results from the article [4] were taken. Different settings and assumptions were investigated as shown in Fig. 6.

The first division of evaluated numerical models was made based on the shape of damaged region created in the composite sample as a result of impact. Cylindrical models assumed that for each ply the damaged region is exactly the same. However for each ply, as proved in the article [13], the region influenced by the impact (deteriorated material properties or delamination) displays evident tendency to grow with the smallest area being characteristic for the impacted side. This conical behaviour was mimicked by changing a diameter of the damaged area along the thickness of the plate (see Fig. 7).

The Delamination Position (DP) parameter specified the location of delamination counted from the bottom of the plate e.g. DP = I meant that separation is present between the first and the second ply when counted from the bottom of the sample (see Fig. 8. for detailed explanation). For cylindrical model all 15 possible cases was calculated while conical configuration was limited to 3 most probable cases (DP = I, II and III).

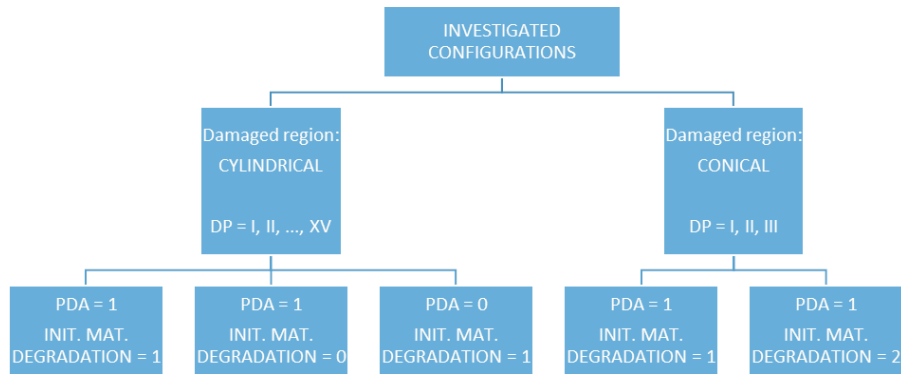


Figure 6 Summary of investigated configurations of the prepared numerical model

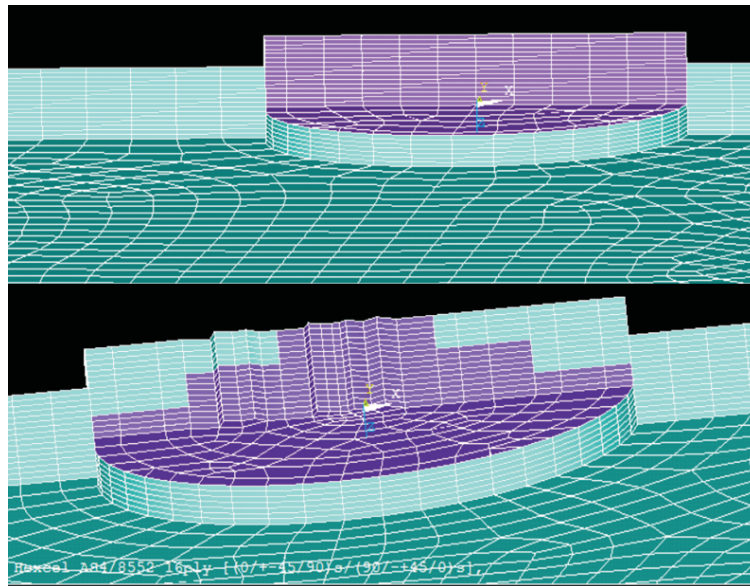


Figure 7 Visualization of cylindrical (TOP) and conical (BOTTOM) damaged zone modelled by the prepared numerical model

In Fig. 7 it may be noticed that elements inside the damaged region are shifted along z axis with respect to rest of the plate. Purpose of such a behaviour was to separate elements located above and below the delamination. It is realized by a proper connection of elements – each element has 3 nodes on each side, nodes

located outside damaged region use their middle node to connect with elements inside. Nodes above the delamination use their lower node, whereas ones located below use a top one. Scheme of this connection is presented in Fig. 8. In this solution delamination is always located on the mid-plane of the elements outside damaged region. Each element has 3 nodes on each side (8 in total) marked with dots. Green dots represent common nodes for all three parts, whereas red ones all remaining nodes. Should the different approach have been used, elements above and below delamination would be located in the same space what would result in having different elements located in the same space.

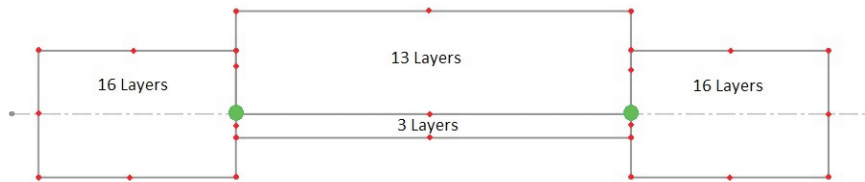


Figure 8 Scheme of the nodes connection allowing to properly define delamination position

For each value of parameter DP in cylindrical model, two other aspects were considered: the influence of progressive damage analysis and material properties within damaged region. If non-linear progressive damage analysis was turned off (PDA = 0), Hashin failure criterion was applied to evaluate which elements were destroyed for investigated loading. What is more, cases where delamination was the only negative result of the impact (material properties assumed to remain unchanged; INIT. MAT. DEGRADATION = 0) were checked.

All configurations for conical model were solved with utilization of Progressive Damage Analysis and deteriorated material properties. Additionally, one extra set of material properties for damaged region was evaluated (INIT. MAT. DEGRADATION = 2). Applied material properties for damaged region are listed in Tab. 4.

Table 4 Deteriorated material properties used for damaged region modelling

INIT. MAT. DEGRADATION	E_X [GPa]	E_Y [GPa]	E_Z [GPa]	G_{XY} [GPa]	G_{YZ} [GPa]	G_{XZ} [GPa]	ν
1	6.15	0.52	0.52	0.47	0.47	0.47	0.45
2	12.30	1.04	1.04	0.94	0.94	0.94	0.40

3. Results and findings

The source article [4] indicates, that considered plates broke during compression test under loading in range between 39 and 43 kN. Simulations were evaluated by

comparison of obtained critical load, with that range of load. Critical load refers to the value of compressive force for which first signs of material damage were visible in numerical model.

3.1. CASE 1: Cylindrical damaged zone

Comparison of experimental results from the paper [4], with numerical results obtained for cylindrical damage model is presented in Fig. 10, where MIN and MAX refer to minimum (39 kN) and maximum (43 kN) critical loads from the experiment. For easier evaluation of results, Fig. 9. presents details on delamination positions (Roman numerals), and layer arrangement combined (Theta) for plate impacted at L1. For specimen impacted at L16 delamination position is numbered in reversed order (delamination XV always next to impacted layer).

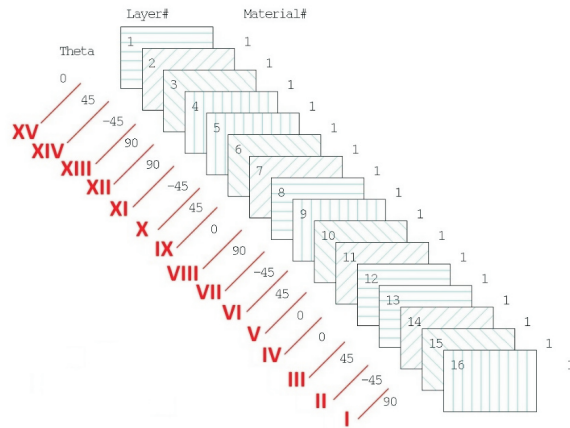


Figure 9 Numeration of delamination positions for plate impacted at L1

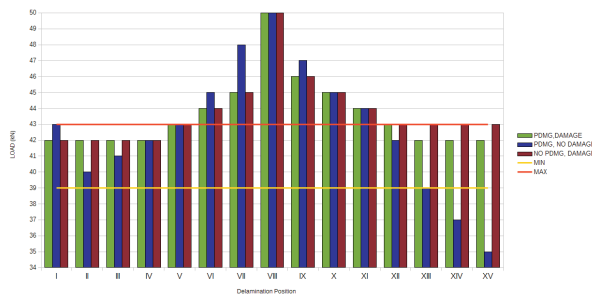


Figure 10 Critical forces for the cylindrical-damaged-zone model compared with experimental data from [3]

Indexes of layers with visible damaged regions for calculated critical loads are presented in Tab. 5 and 6. Tab. 5 shows a comparison for three investigated configurations (as shown in Fig. 6), and Tab. 6 presents results for options differing by damping parameter value only.

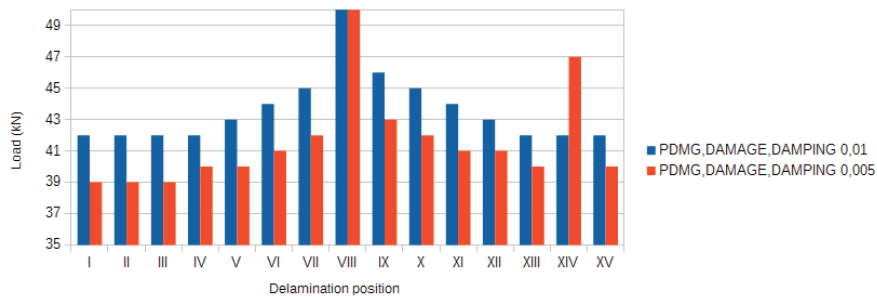


Figure 11 Influence of damping factor on the detected critical force

Additional simulation was performed in order to analyse the influence of damping. It was carried out for the case with enabled PDMG, and damaged material in the delamination region. Value of damping was decreased to 0.005, and was compared with the results from previous simulations performed with damping factor of 0.01. As presented in Fig. 11, damping has noticeable influence; increase in the DF value yielded higher critical force.

3.2. CASE 2: Conical Damaged Zone

In this case, deteriorated material properties for damaged region was changed to Table 4 (*INIT. MAT. DEGRADATION = 2*). Elsewhere, values corresponding to *INIT. MAT. DEGRADATION = 1* were applied.

Table 5 Damaged layers for different cylindrical configurations

<i>Delamination Position DP</i>	<i>PDA = 1 DAMAGE</i>	<i>PDA = 1 NO DAMAGE</i>	<i>PDA = 0 DAMAGE</i>
I	1	1	1
II	1	1	1
III	1	1	1
IV	1	1	1
V	1	1	1
VI	1	1	1
VII	1	1	1
VIII	-	-	-
IX	1, 12, 13	1	13
X	1,2,3,8,12,13	1	12,13
XI	1,2,3,8,12,13	1	12,13
XII	1,2,3,4,5,6,7,8,13	1,2,3,4,16	13
XIII	1	1,2,3,16	12,13
XIV	1	1,2,16	12,13
XV	1,2,3,8	1	12,13

Table 6 Destroyed layers for different damping values

<i>Delamination Position DP</i>	<i>PDA = 1 DAMAGE DAMPING = 0.01</i>	<i>PDA = 1 DAMAGE DAMPING = 0.005</i>
I	1	1
II	1	1
III	1	1
IV	1	1
V	1	1
VI	1	1
VII	1	1
VIII	-	-
IX	1,12,13	1,12,13
X	1,2,3,8,12,13	1,12,13
XI	1,2,3,8,12,13	1,13
XII	1,2,3,4,5,6,7,8,13	1,2,3,12,13
XIII	1	1,2,3,13
XIV	1	1,13
XV	1,2,3,8	1,13

Table 7 Damaged layers for different conical configurations

<i>Delamination Position DP</i>	<i>Impacted side</i>	<i>Critical Force [kN]</i>	<i>Corresponding Damaged Layer</i>
I	L1	20	1
	L16	24	12
II	L1	20	1
	L16	24	12
II*	L1	23	1
	L16	28	12
III	L1	20	1
	L16	23	12

It must be noted that the resolution of all simulations was 1 kN what might have been too low to find the precise results concerning destroyed plies. It is presumed that if the resolution was increased it would be possible to find a more precise value of critical load, for which only one ply would indicate damage.

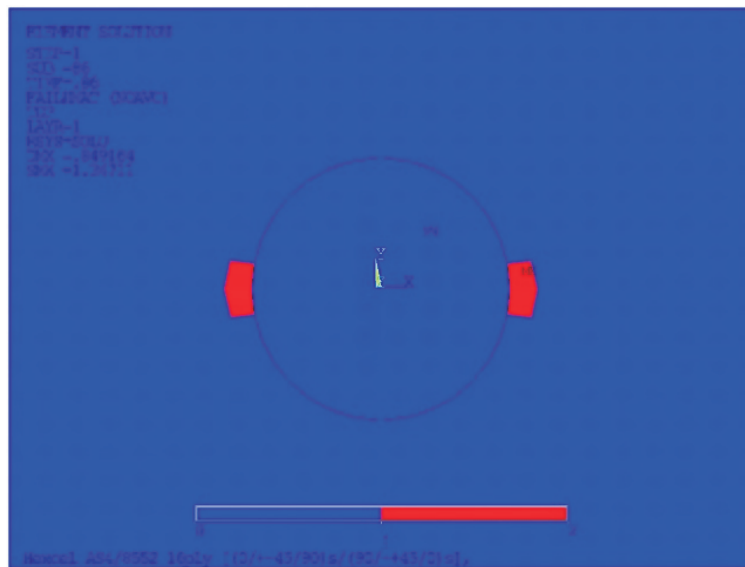


Figure 12 Damaged region for cylindrical model with damaged material in delamination position, represented by Hashin criterion

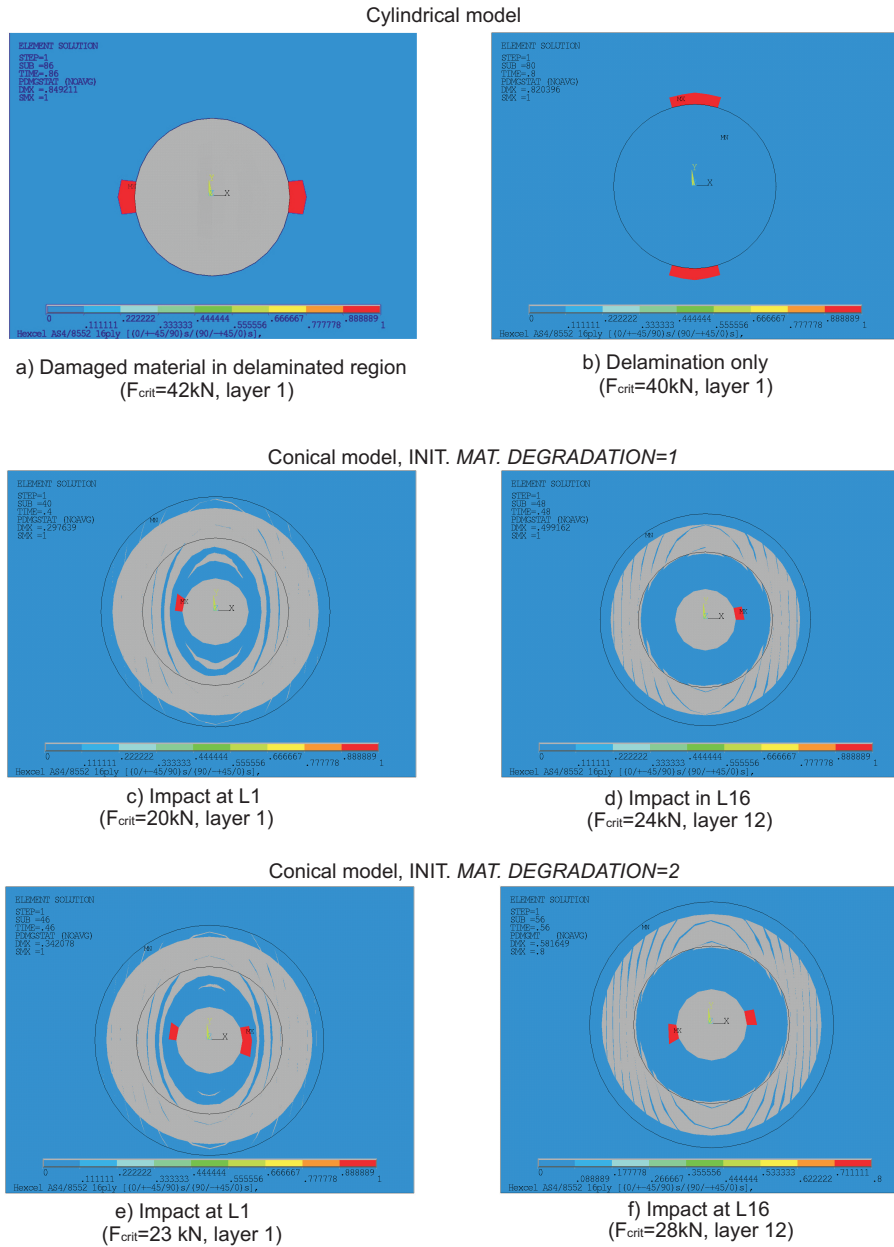


Figure 13 Comparison of PDA results obtained for critical forces

Fig. 13. presents a comparison of PDA results from all investigated cases. All pictures show behaviour of the ply, which was damaged as the first in each case (First Ply Failure criterion). Blue colour indicates then intact material, red colour

presents material destroyed during simulation, whereas grey zones represent initially damaged material (during impacting). One case for cylindrical model was examined without PDA, its results were evaluated with Hashin criterion and are presented in Fig. 12.

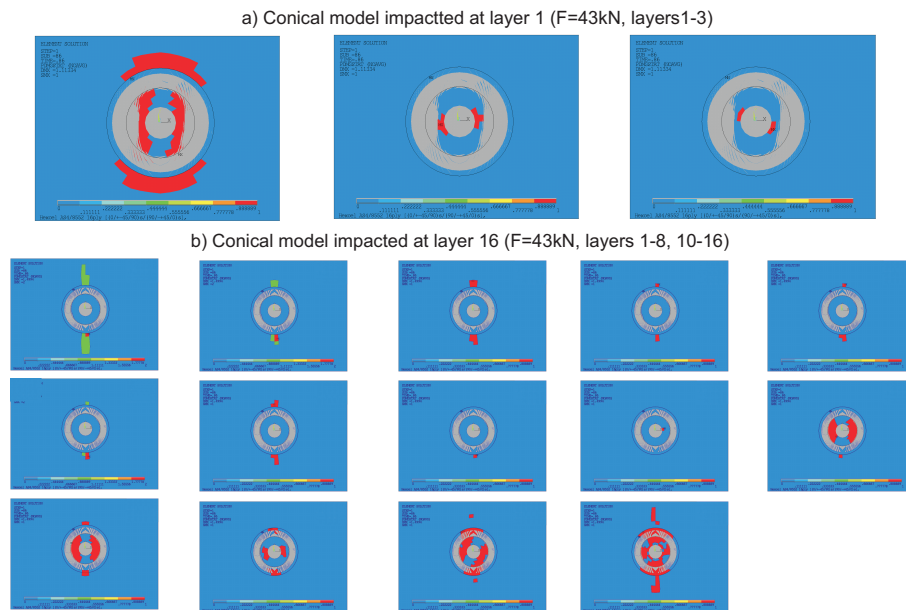


Figure 14 All damaged surfaces for the biggest critical force presented in [4]

As it can be seen in Figs. 12 and 13 – in almost all cases first signs of failure are visible in very similar locations, placed along X axis. The failure is present in form of several destroyed elements on each side of damaged region. Only one case, without damaged material in delaminated region, indicates that damage propagates in different direction – along Y axis. As far as the exact type of damage is concerned, in Fig. 13 b) the circular area is not initially damaged (material is stiffer), so PDA criterion is violated for matrix compression. Contrary, all 5 remaining cases (from Fig. 13) containing initial damage of material, appear to be destroyed in matrix tension. It was caused by the change of circular shape of damaged material into elliptical due to compressive force acting along X axis.

Results shown in Fig. 13 are valid for the critical forces resulting from the simulation. As [4] indicates that plates could withstand a load up to 43 kN, Fig. 14 presents destroyed regions in individual layers for two configurations of conical model, under such a load. Although plates impacted at layer 16 withstand slightly higher critical load than those impacted at layer 1 (see Table 7), it can be noticed that for 43 kN many more layers contain damaged region in the first case. Also in some layers dual failure mode is present, where both matrix and fibres brake (green regions).

Despite the analysis was initially considered to eliminate buckling phenomena (by applying anti-buckling fixture in [4]), it was impossible, which may be seen in Fig. 14. The obtained buckling shape is present in form of three half-waves placed along X axis.

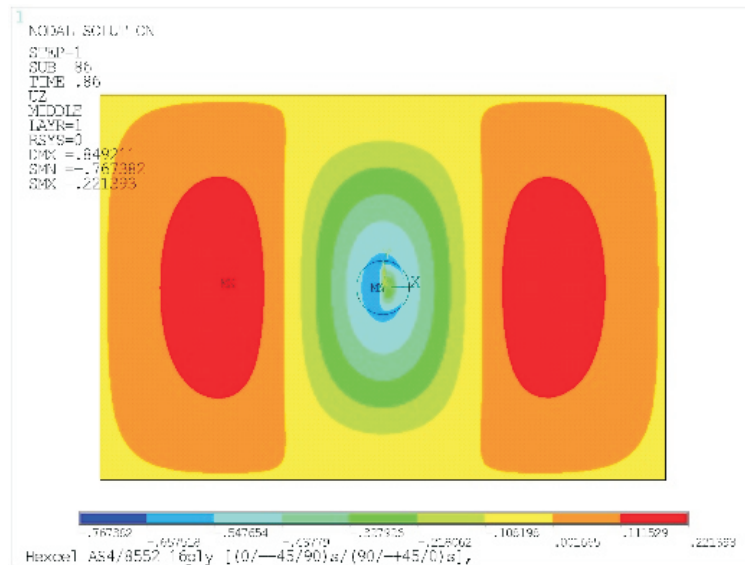


Figure 15 Exemplary displacement of nodes in Z direction (buckling of the plate)

4. Conclusions

Taking above results into consideration one can say that the shape of the damaged zone (through the ply thickness) influences the value of critical force in compression. Conical model of damage should better reflect real behaviour of compressed plate, which comes from [13]. However the model must be properly tuned in order to match experimental result. Such procedure requires to verify the influence of many variables possible to be modified such as: cone shape, destroyed material properties, delamination number and their locations, damping coefficient, size of the damaged region.

As it may be noticed from the comparison between results calculated for different value of damping, the value of this rheological parameter does have strong influence on the value of critical force. Damaging force increases with increasing damping what can be explained by growth of energy dissipated on elastic behaviour.

Acknowledgments

The paper has been written under the research project:

No UMO-2015/17/B/ST8/00033 financed by the National Science Centre Poland.

References

- [1] **Adams, D.:** Testing Tech: Compression After Impact Testing, *High-Performance Composites*, **2007**.
- [2] **Kursun, A., Senel, M. and Enginsoy, H.:** Experimental and numerical analysis of low velocity impact on a preloaded composite plate, *Advances in Engineering Software*, 90, 41–52, **2015**.
- [3] Compression After Impact testing, '<http://www.zwick.com/en/applications/composites/fiber-composites/compression-after-impact.html>', Accessed on **2016**.
- [4] **Sztefek, P. and Olsson, R.:** Nonlinear compressive stiffness in impacted composite laminates determined by an inverse method, *Composites. Part A: Applied Sciences and Manufacturing*, 40, 3, 260–272, **2009**.
- [5] **Aymerich, F. and Priolo, P.:** Characterization of fracture modes in stitched and unstitched cross-ply laminates subjected to low-velocity impact and compression after impact loading, *Journal of Impact Engineering*, 35, 591–608, **2008**.
- [6] **Cartie, D. D. R. and Irving, P. E.:** Effect of resin and fibre properties on impact and compression after impact performance of CFRP, *Composites. Part A*, 33, 483–93, **2002**.
- [7] **Zhang, X., Hounslow, L. and Grassi, M.:** Improvement of low-velocity impact and compression-after-impact performance by z-fibre pinning, *Composites Science and Technology*, 66, 2785–2794, **2006**.
- [8] **Li, N. and Chen, P. H.:** Micro-macro FE modelling of damage evolution in laminated composite plates subjected to low velocity impact, *Composite Structures*, 147, 111–121, **2016**.
- [9] **Schwab, M., Todt, M., Wolfahrt, M. and Pettermann, H. E.:** Failure mechanism based modelling of impact on fabric reinforced composite laminates based on shell elements, *Composites Science and Technology*, 128, 131–137, **2016**.
- [10] **Dębski, H., Kubiak, T. and Teter, A.:** Buckling and postbuckling behaviour of thin-walled composite channel section column, *Composite Structures*, 100, 195–204, **2013**.
- [11] **Harvey, S.:** Composites Seminar 2012, Seattle, **2012**.
- [12] ANSYS Inc.: ANSYS Mechanical APDL Structural Analysis Guide, Release 15.0, **2013**.
- [13] **Petit, S., Bouvet, C., Bergerot, A. and Barrau, J-J.:** Impact and compression after impact experimental study of a composite laminate with a cork thermal shield, *Composites Science and Technology*, 67, 3286–3299, **2007**.
- [14] **Barbero, E. J., Cosso, F. A., Roman, R. and Weadon, T. L.:** Determination of material parameters for Abaqus progressive damage analysis of E-glass epoxy laminates, *Composites*, 46, 211–220, **2013**.

